Supporting Information

Order-disorder transition involving the A-site cations in $Ln^{3+}Mn_3V_4O_{12}$ perovskites

Yuichi Shimakawa,[†,‡,*] Shoubo Zhang,[†] Takashi Saito,[†] Michael W. Lufaso,[§] and Patrick M. Woodward[‖]

[†]*Institute for Chemical Research, Kyoto University, Gokasho, Uji, Kyoto 611-0011, Japan*
[‡]*Japan Science and Technology Agency, CREST, Uji, Kyoto 611-0011, Japan*
[§]*Department of Chemistry, University of North Florida, 1 UNF Drive, Jacksonville, FL 32224, USA*
[‖]*Department of Chemistry, Ohio State University, 100 West 18th Avenue, Columbus, OH 43210, USA*

This supporting information includes 8 figures and 5 tables.

[*]e-mail: shimak@scl.kyoto-u.ac.jp

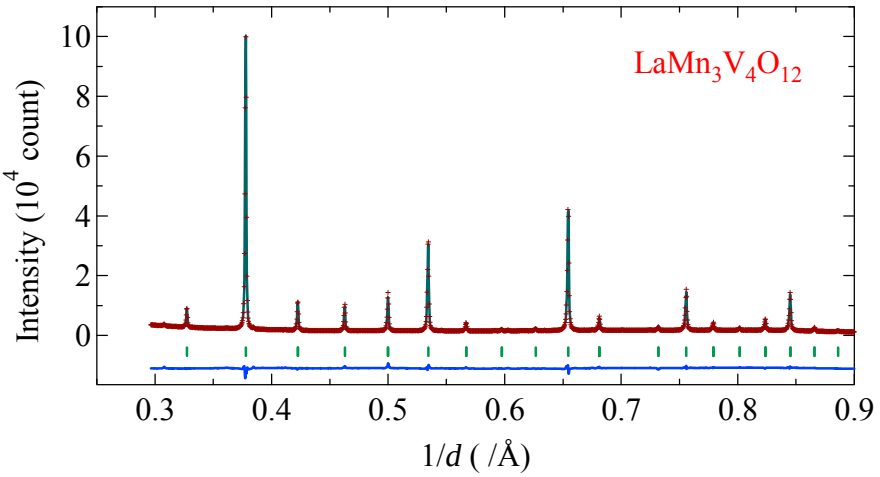

Figure S1 Synchrotron XRD patterns and the structure refinement results for $LaMn_3V_4O_{12}$. The observed (marks), calculated (line), and difference (bottom line) patterns are shown. The ticks indicate the positions of Bragg reflections.

Table S1 Refined structure parameters for $LaMn_3V_4O_{12}$ from the Rietveld analysis of synchrotron XRD data. g is the occupation factor and B is the isotropic thermal parameter. Numbers in parentheses are standard deviations of the last significant digit. Space group: $Im\bar{3}$. a = 7.4830(1) Å, R_{wp} = 4.96%, R_p = 3.87%, R_e = 2.40%, and S = 2.07.

Atom	Site	X	y	z	G	B (Å^2)
La	2*a*	0.0	0.0	0.0	1.0	0.12(2)
Mn	6*b*	0	0.5	0.5	1.0	1.85(4)
V	8*c*	0.25	0.25	0.25	1.0	0.25(2)
O	24*g*	0.0	0.1954(4)	0.2941(5)	1.0	1.0

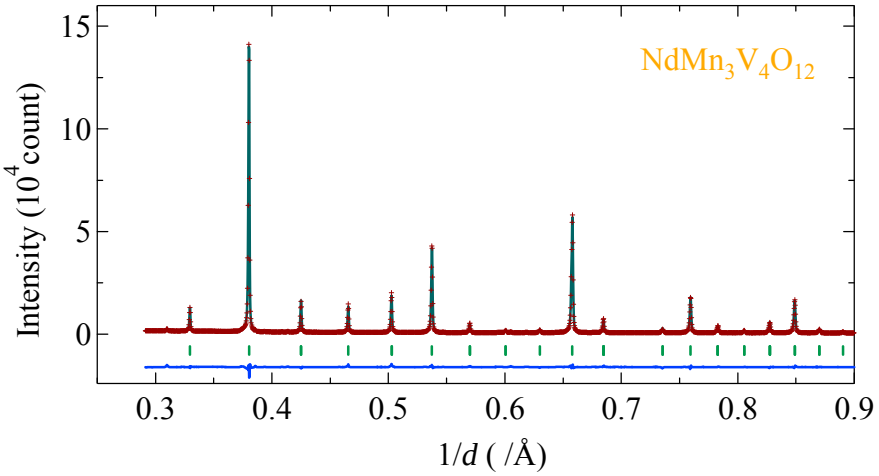

Figure S2 Synchrotron XRD patterns and the structure refinement results for $NdMn_3V_4O_{12}$. The observed (marks), calculated (line), and difference (bottom line) patterns are shown. The ticks indicate the positions of Bragg reflections.

Table S2 Refined structure parameters for $NdMn_3V_4O_{12}$ from the Rietveld analysis of synchrotron XRD data. g is the occupation factor and B is the isotropic thermal parameter. Numbers in parentheses are standard deviations of the last significant digit. Space group: $Im\bar{3}$. a = 7.4596(1) Å, R_{wp} = 4.94%, R_p = 3.51%, R_e = 2.78%, and S = 1.77.

Atom	Site	*X*	*y*	*z*	*G*	*B* (Å^2)
Nd	2*a*	0.0	0.0	0.0	1.0	0.32(1)
Mn	6*b*	0	0.5	0.5	1.0	1.73 (2)
V	8*c*	0.25	0.25	0.25	1.0	0.37(1)
O	24*g*	0.0	0.1930(3)	0.2904(3)	1.0	1.0

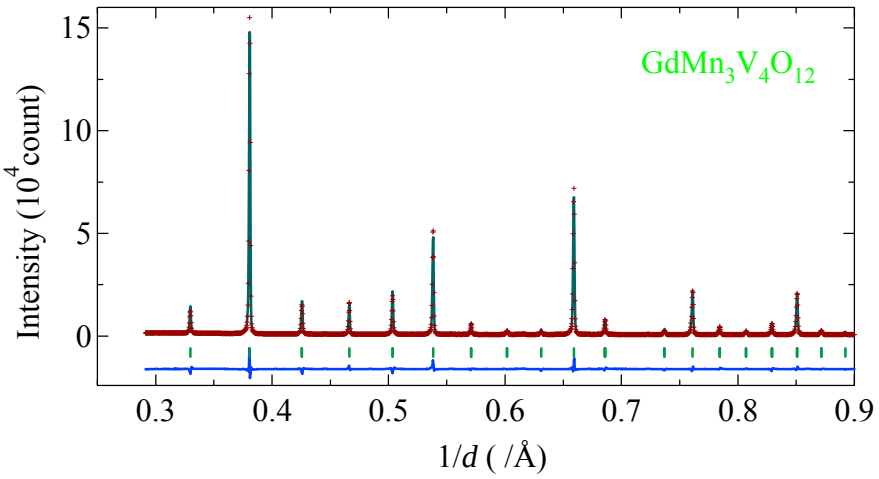

Figure S3 Synchrotron XRD patterns and the structure refinement results for $GdMn_3V_4O_{12}$. The observed (marks), calculated (line), and difference (bottom line) patterns are shown. The ticks indicate the positions of Bragg reflections.

Table S3 Refined structure parameters for $GdMn_3V_4O_{12}$ from the Rietveld analysis of synchrotron XRD data. *g* is the occupation factor and *B* is the isotropic thermal parameter. Numbers in parentheses are standard deviations of the last significant digit. Space group: *Im*–3. a = 7.4403(1) Å, R_{wp} = 6.19%, R_p = 4.51%, R_e = 2.69%, and S = 2.30.

Atom	Site	*X*	*y*	*z*	*G*	*B* (Å^2)
Gd	2*a*	0.0	0.0	0.0	1.0	0.70(1)
Mn	6*b*	0	0.5	0.5	1.0	1.17 (2)
V	8*c*	0.25	0.25	0.25	1.0	0.25(1)
O	24*g*	0.0	0.1913(3)	0.2861(3)	1.0	1.0

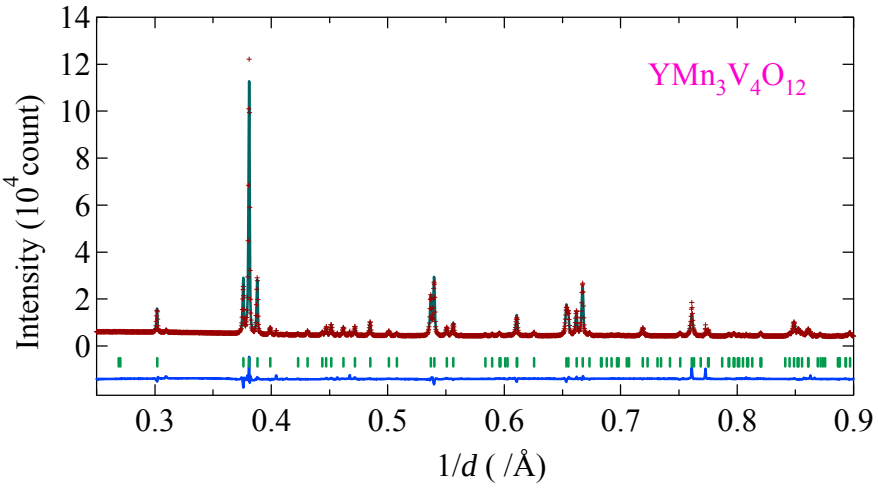

Figure S4 Synchrotron XRD patterns and the structure refinement results for $YMn_3V_4O_{12}$. The observed (marks), calculated (line), and difference (bottom line) patterns are shown. The ticks indicate the positions of Bragg reflections.

Table S4 Refined structure parameters for $YMn_3V_4O_{12}$ $[(Y_{1/4}Mn_{3/4})VO_3]$from the Rietveld analysis of synchrotron XRD data. *g* is the occupation factor and *B* is the isotropic thermal parameter. Numbers in parentheses are standard deviations of the last significant digit. Space group: *Pnma*. a = 5.3328(2) Å, b = 7.4624(3) Å, a = 5.1667(2) Å, R_{wp} = 3.14%, R_p = 1.91%, R_e = 1.43%, and S = 2.19.

Atom	Site	*X*	*y*	*z*	*G*	*B* (Å^2)
Y	4*c*	0.0537(2)	0.25	0.4886(3)	0.25	0.56(3)
Mn	4*c*	0.0537(2)	0.25	0.4886(3)	0.75	0.56(3)
V	4*a*	0.0	0.0	0.0	1.0	0.28(3)
O1	4*c*	0.4534(9)	0.25	0.6112(8)	1.0	1.0
O2	8*d*	0.2951(7)	0.0531(5)	0.1924(7)	1.0	1.0

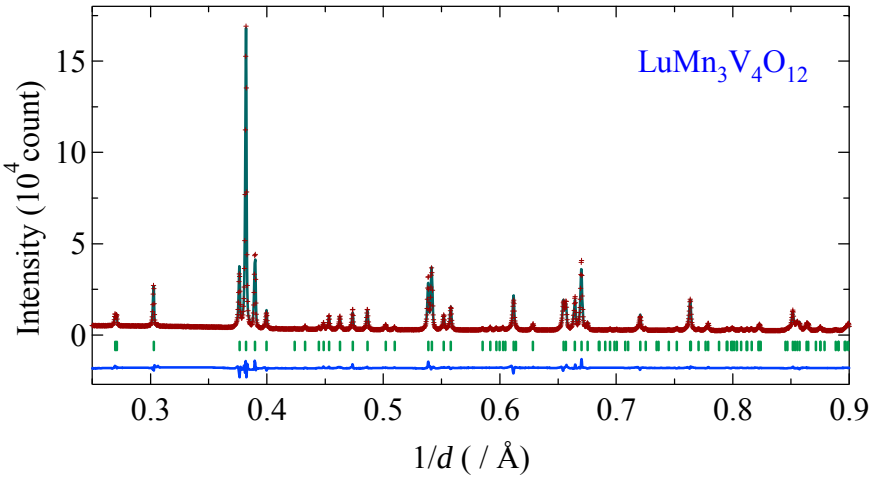

Figure S5 Synchrotron XRD patterns and the structure refinement results for $LuMn_3V_4O_{12}$. The observed (marks), calculated (line), and difference (bottom line) patterns are shown. The ticks indicate the positions of Bragg reflections.

Table S5 Refined structure parameters for $LuMn_3V_4O_{12}$ [$(Lu_{1/4}Mn_{3/4})VO_3$] from the Rietveld analysis of synchrotron XRD data. *g* is the occupation factor and *B* is the isotropic thermal parameter. Numbers in parentheses are standard deviations of the last significant digit. Space group: *Pnma*. a = 5.3250(1) Å, b = 7.4396(2) Å, a = 5.1415(1) Å, R_{wp} = 4.30%, R_p = 3.19%, R_e = 1.65%, and S = 2.60.

Atom	Site	*X*	*y*	*z*	*G*	*B* (Å^2)
Lu	4*c*	0.0592(1)	0.25	0.4860(2)	0.25	0.35(2)
Mn	4*c*	0.0592(1)	0.25	0.4860(2)	0.75	0.35(2)
V	4*a*	0.0	0.0	0.0	1.0	0.28(2)
O1	4*c*	0.4527(8)	0.25	0.6121(7)	1.0	1.0
O2	8*d*	0.3006(6)	0.0538(4)	0.1911(6)	1.0	1.0

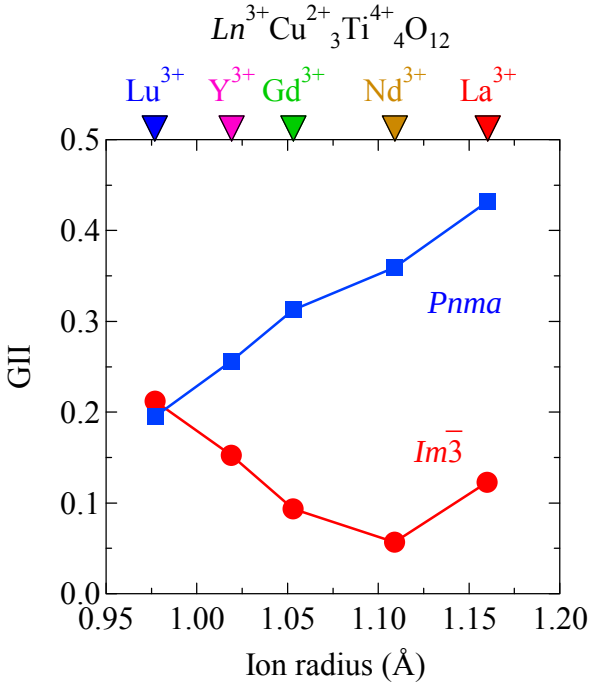

Figure S6 Calculated GII for hypothetical $Ln^{3+}Cu^{2+}{}_3Ti^{4+}{}_4O_{12}$ as a function of A-site Ln^{3+} ion radius. Note that the actual compounds have chemical compositions of $Ln^{3+}{}_{2/3}Cu^{2+}{}_3Ti^{4+}{}_4O_{12}$. Because the *SPuDS* program cannot calculate GII for the compounds with vacancies, the tentative results for those non-charge-neutral compositions are presented. Even though, it is clear that the $Ln^{3+}{}_{2/3}Cu^{2+}{}_3Ti^{4+}{}_4O_{12}$ compounds do not crystallize with the A-site-disordered *Pnma* simple-perovskite structures.

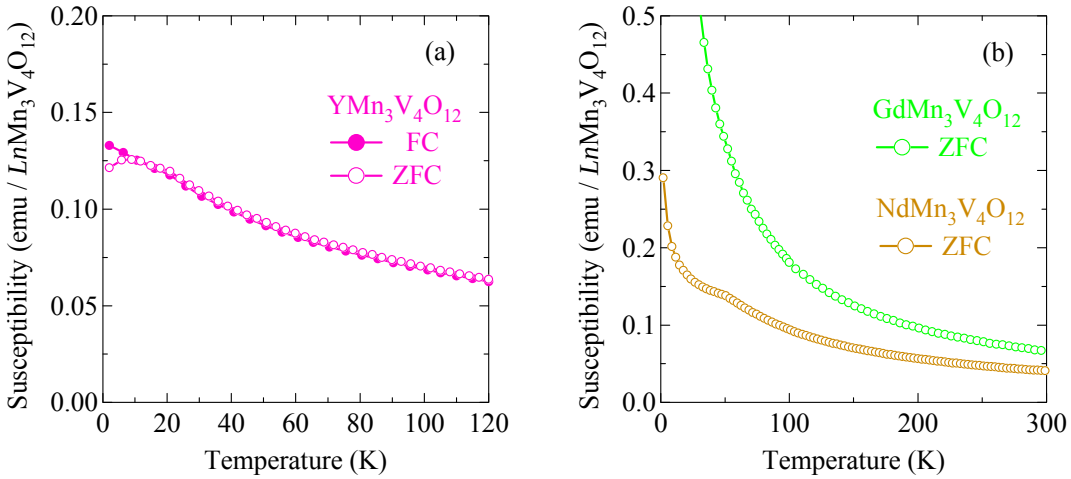

Figure S7 (a) Temperature dependence of magnetic susceptibility measured under ZFC (open symbols) and FC (closed symbols) for A-site-disordered simple-perovskite $YMn_3V_4O_{12}$. A spin-glass-like magnetic behavior is observed similar to $LuMn_3V_4O_{12}$. (b) Temperature dependence of magnetic susceptibility measured under 1-kOe ZFC for A-site-ordered double-perovskite $NdMn_3V_4O_{12}$ and $GdMn_3V_4O_{12}$. Antiferromagnetic transitions are not clearly seen in the magnetic susceptibility measurements, because of the large contribution of the A-site Nd^{3+} and Gd^{3+} moments.

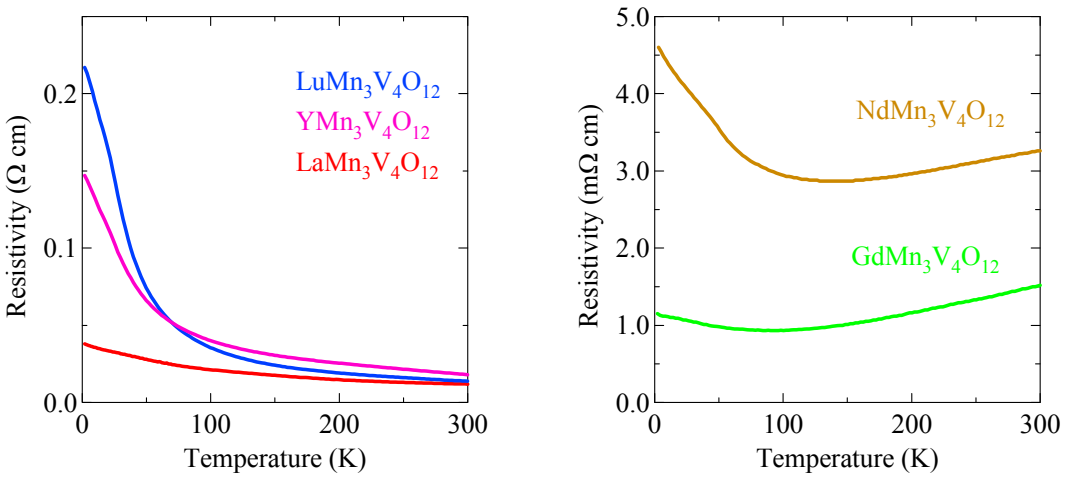

Figure S8 Temperature dependence of resistivity for LnMn$_3$V$_4$O$_{12}$ (Ln = La, Nd, Gd, Y, Lu). Although some grain boundary effects may prevent the samples from having the metallic behaviors, low resistivity, which is less than a few hundreds mΩ cm even at low temperatures, suggests the delocalization of electrons.